Particle Accelerators
1973, Vol. 5, pp. 199–206

THE GEOMETRY AND OPTICS OF SYNCHROTRON RADIATION†

A. P. SABERSKY

Stanford Linear Accelerator Center, Stanford University, Stanford, California 94305, USA

The geometrical–optical properties of synchrotron radiation coming from a curving, relativistic electron beam do not fit into any usual category of light or radiation source. The center of the apparent source of radiation depends on the position of the observer with respect to the orbit, and the source has an axial extent which is a function of the sizes of the beam and the observation aperture. The beam image formed by focusing the synchrotron light is subject to distortions and depth of field errors. These errors are calculated, and, in some cases, methods of correction are given. The limits put on resolution by geometrical effects are given. Beam orbit changes cause errors in the angular acceptance of observation systems: these effects can also be corrected. The dimensions of the diffuse shadows cast by rays from the finite-sized source impinging on edges are calculated.

1. INTRODUCTION

In high energy electron accelerators and storage rings, synchrotron radiation gives the machine designer many problems, and solves a few. This paper gives derivations of the properties of synchrotron light interesting to those who use synchrotron light to study electron beams in extent and intensity, and those who use the synchrotron light itself as a tool.

An excellent review of synchrotron radiation properties has been presented by R. P. Godwin[1]; there is also a careful analytical treatment in the book by Sokolov and Ternov.[2] Some of the problems of imaging and using synchrotron radiation have been treated by Tomboulian and Hartman.[3]

2. GEOMETRIC PROPERTIES

We concern ourselves with the problem of an observer at a point struck by synchrotron radiation. What point on the electron orbit illuminates the observation point, and how is the location of the emission point to be defined?

We first represent the electron beam as a single line and the emitted radiation as rays tangent to a curved orbit. We deal only with orbits in uniform magnetic fields and field-free spaces throughout. The observation point is in a field-free region adjacent to a sharply bounded bending field, in the plane of the bend. The geometry of the problem is shown in Figure 1. In Appendix A, we derive equations for the emission distance l and the angle with respect to the local straight trajectory, 2δ.

$$\delta = \tan^{-1}\left[\frac{-l_0-(l_0^2+d(2R+d))^{1/2}}{2R+d}\right]$$

$$\approx \frac{-l_0-[l_0^2+2dR]^{1/2}}{2R} \qquad \text{for small } \delta \text{ and } R \gg d$$

$$l = \frac{d}{\sin 2\delta} + R\tan\delta \approx \frac{d}{2\delta} + R\delta$$

where the independent variables are:

R = the radius of bend
l_0 = the distance from the end of the curved orbit to a perpendicular from the observation point
d = the perpendicular distance from the observation point to the straight trajectory.

If one is using these equations in the design of synchrotron radiation shields or other systems it is very convenient to plot sets of solutions on a graph for reference.

When the orbit of the electron beam moves radially, the emission point moves also. We look

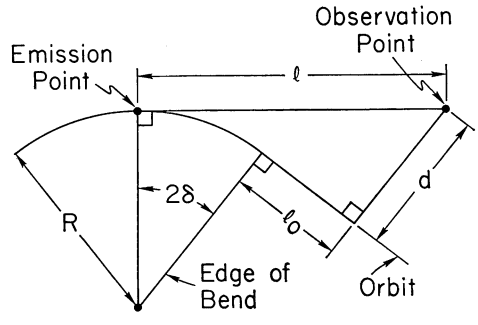

FIGURE 1 Basic geometry of synchrotron radiation emission and observation.

† Work supported by the U.S. Atomic Energy Commission.

at the case in which the orbit moves perpendicular to itself at the original emission point. For $\cos 2\delta \approx 1$, the changes in orbit position can be expressed as changes in d.

The change in emission distance, l, with d is given by

$$\frac{\partial l}{\partial d} = \frac{R(l_0 + k^{1/2} - d \cdot R \cdot k^{-1/2})}{(l_0 + k^{1/2})^2} - R \cdot k^{-1/2}$$

$$k = l_0^2 + 2dR.$$

This quantity defines the slope of a line of emission points with respect to the original observation axis (Figure 2). If $\partial^2 l/\partial d^2 \ll \partial l/\partial d$ in the region

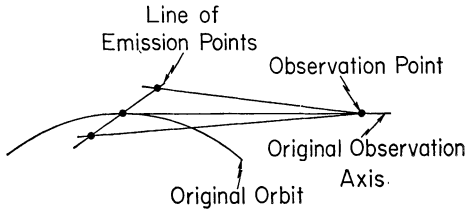

FIGURE 2 Definition of the optical axis and line of emission points.

of interest, $\partial l/\partial d$ can be considered a constant. $\partial\delta/\partial d$ can be treated similarly.
For the full emission angle, $\gamma = 2\delta$

$$\frac{\partial \gamma}{\partial d} = (l_0^2 + 2\,dR)^{-1/2} \qquad \tan 2\delta \cong \gamma.$$

Since l changes with d, the horizontal angular acceptance of an aperture at the observation point also changes with orbit displacements. The fractional change in aperture angle, $\alpha = s/l$ (Figure 12), for a displacement Δd is:

$$\frac{\Delta\alpha}{\alpha} = -\frac{\Delta d}{l}\frac{\partial l}{\partial d} \qquad \Delta d \frac{\partial l}{\partial d} \ll l.$$

This effect may be troublesome in photometric work. A method of correction is given in Appendix B.

3. BEAM IMAGE: HORIZONTAL COMPONENT

A curved particle beam emitting a collimated cone of light tangent to its curvature is an unusual object for optical observation. We use the phase-space techniques commonly applied to charged particle optics[4] for analysis. We assume that defining apertures are rectangular, so that the ray optics can be treated separately in the horizontal and vertical planes.

Following the geometrical analysis of the previous section, we first treat a line beam emitting a single ray tangent to its curvature. We leave out the dependence of angle on time and assume that our observation system looks at all rays for all time. The optical axis is the ray passing through the center of the observation aperture (Figure 3).

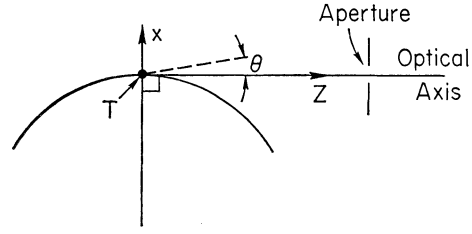

FIGURE 3 Coordinates for phase space representation of the light source.

The tangent point, T, is the point $x = 0$, $z = 0$, and angles are referred to the z axis, as shown. For example, we look at two points on opposite sides of T, T_1 and T_2 at an angle δ (Figure 4). The tangent

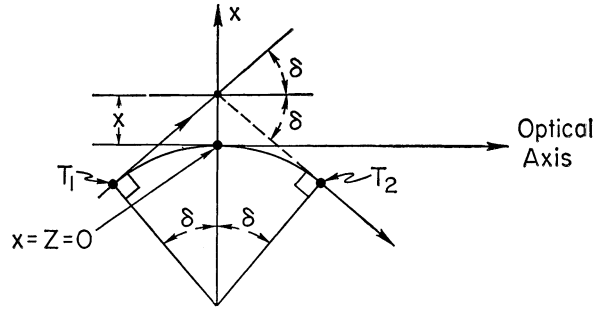

FIGURE 4 Projection of tangent rays to the source plane.

at T_1 is projected forward to the $z = 0$ line, and the tangent at T_2 is projected backwards. All tangents are similarly projected to $z = 0$. For small θ, the trace of the tangents on the $x-\theta$ plane at $z = 0$ is expressed by (see Figure 5):

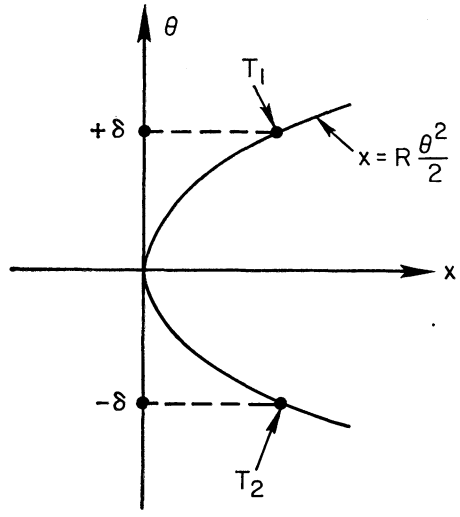

FIGURE 5 Phase-space representation of the light source at $z=0$.

$$x=\tfrac{1}{2}R\theta^2.$$

It is desirable to work at $z=0$ because a linear transformation of this trace to another z results in a very complex function.

When a beam of electrons with a finite size, $\pm x_{03}$, and zero divergence is centered on the line beam of the previous section, the rays it emits fill an area whose boundaries are parallel to the original central ray line (Figure 6). This area will be referred to as the source area.

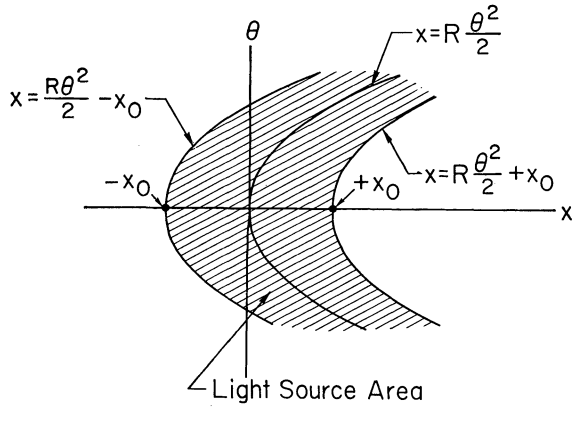

FIGURE 6 Light source area.

Visible synchrotron light has a divergence angle in the horizontal plane, typically milliradians for ultrarelativistic electrons. The particle beam also has a finite divergence.† The total light divergence angle, θ_{tot}, is usually given as the quadratic sum of these two divergences. The total divergence has no effect on the intensity distribution in the source area if

$$\tfrac{1}{2}R\theta_{\text{tot}}^2 \ll x_0.$$

We treat only this case.

A restricting aperture forms a pair of lines parallel to the θ axis in phase space. The aperture edges can be transformed backwards or forwards along the optical axis to any other point, where they will also appear as a pair of parallel straight lines. We define an aperture $\pm a$ wide, symmetrical about the optical axis. The equations of the edges are, for the $+a$ and $-a$ edges, respectively,

$$x-a=0,$$
$$x+a=0.$$

Transformed backwards a distance l along the Z axis, the equations of the edges are

$$\theta+(x-a)/l=0,$$
$$\theta+(a-x)/l=0.$$

The two edges of the observation aperture, transformed back to the emission point, are superimposed on the source area (Figure 7). In this case, the aperture size ($\pm a$), is smaller than the beam size ($\pm x$).

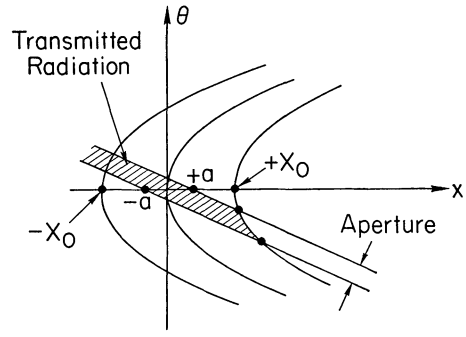

FIGURE 7 A distant aperture transformed backwards onto the source area.

We can now define exactly the boundaries of the source area seen through the aperture, and we need to know how accurately this source represents the horizontal beam cross section. A typical optical

† We assume that the beam divergence is small enough so that its size is constant in the region of interest.

observation device, such as a television camera or photographic film, looks at the intensity distribution in one plane perpendicular to the optical axis. All information about angular distribution or x, θ correlation is lost in this process. What we see is the projection of the distribution in (x,θ) onto the x axis.

If the beam were an ordinary self-luminous object, the boundaries of the light source area would be straight, parallel to the θ axis and symmetrical about $x = 0$.

However, looking at Figure 7 as an example, we can see errors due to curvature and asymmetry of the source area boundaries. The magnitude of the error is approximately equal to the difference between x_0 and the projections of the four intersection points onto the x axis. An approximation to the total error, Δx_0, is given by

$$\Delta x_0 = R\left(\frac{x_0 + a}{l}\right)^2.$$

If $\Delta x_0 \ll x_0$, we may forget about the distortions. Note that as the quantity a becomes very small, Δx_0 does not go to zero.

If the distortions are a problem, they can be partially compensated with second-order optics (Appendix C) or improved by increasing l.

The treatment so far has been geometrical, and one must include diffraction effects when dealing with small horizontal apertures.

4. SHADOW EFFECTS

If the observation point is an edge, such as a protection collimator, the synchrotron radiation casts a shadow whose edge is tangential to the beam orbit (Figure 8). The distribution of electrons in a real beam causes a penumbra to extend beyond the straight shadow edge cast by a line beam. The angular power distribution in the penumbra is related to the radial power distribution in the beam, exactly as the shadow angle is related to radial orbit displacements. The power distribution in a penumbra radially outward from an edge is determined by the beam power distribution radially inside the beam center line. For a radial beam current distribution $P(r)$ the angular penumbral power distribution is

$$P(\text{angular}) = P(r)\,\partial\gamma/\partial d.$$

For a Gaussian beam current distribution with standard deviation width x, the total power in the penumbra is

$$P(\text{penumbra}) = 1.25\,P_\theta\,\partial\gamma/\partial d,$$

where P_θ is the power per radian in the synchrotron radiation.

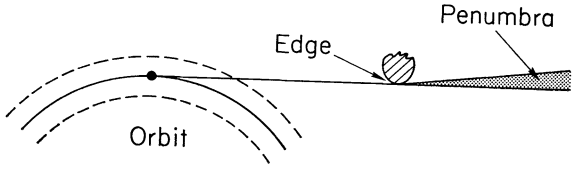

FIGURE 8 Shadow effects due to finite beam size.

5. BEAM IMAGE—VERTICAL

In this section we derive the vertical resolution of an ideal optical system used to observe the electron beam by its emitted light. Since the emission properties of the beam determine the ultimate resolution limit, rather than the properties of the optical system, we shall always refer to the resolution in object space.

An electron beam emitting synchrotron radiation is a self-collimated luminous object. The angular divergence of the light in the vertical plane is a function of the bending radius and the energy of the electron beam. A useful, precise tabulation of synchrotron light properties can be found in Ref. 5. The ultimate vertical resolution in the image is determined by the vertical angular divergence of the light, ϕ:

$$\delta y_1 \approx \lambda/\phi$$

δy = resolution
λ = light wavelength
ϕ = angular width.

The visible synchrotron radiation is elliptically polarized, the angular distributions being quite different for the components perpendicular or parallel to the plane of bend.[6] Thus, the angular distribution of the light can be modified by using

polarization analyzers in front of the optical system used to image the light.

The electron beam has a finite divergence,[7] and this should be properly added to the light divergence angle, for resolution and depth of field calculations; however, the beam divergence is usually small compared to the light divergence angle, and will be ignored.

For a beam with horizontal size x_0, each edge of the horizontal aperture defines a line which is a boundary of the horizontal emission area (Figure 9).

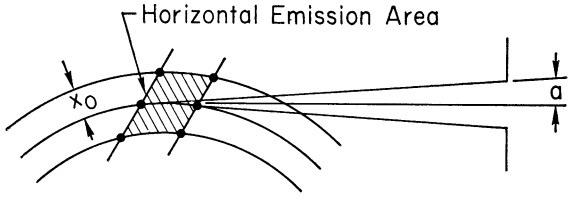

FIGURE 9 Horizontal emission area of a beam observed through an aperture.

The other two edges have the curvature of the orbit. The angle subtended by an aperture of size a is

$$\theta = a\frac{\partial\theta}{\partial d}$$

Thus, the length of arc forming the curved boundary is

$$C = R\cdot a\cdot\frac{\partial\theta}{\partial d}.$$

Treating the emission area as a parallelogram, the effective z extent of the horizontal emission area can be expressed, for small θ, as

$$\delta z = x_0\frac{\partial l}{\partial d} + R\cdot a\cdot\frac{\partial\theta}{\partial d}.$$

The depth field of error is

$$\delta y_2 = \delta z\cdot\phi \ .$$

If all distributions of angle and intensity are Gaussian, the vertical resolution is given by

$$\delta y = [(\delta y_1)^2 + (\delta y_2)^2]^{1/2}.$$

For a more exact formulation of the depth-of-field problem, one must consider the effect of the sharp edges of the emission area due to the aperture edges differently from the 'soft' edges due to the beam-intensity distribution.

It is interesting that the vertical resolution depends on horizontal beam size and horizontal aperture.

It is possible to reduce the effect due to the beam horizontal size by placing a horizontal image stop in the image plane of the optical instrument (Figure 10). The restricted image can be refocused or the

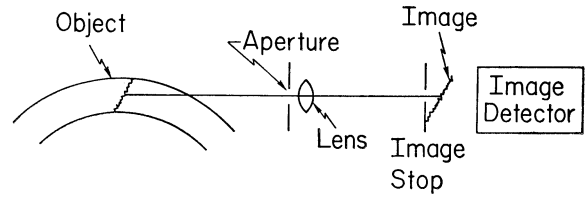

FIGURE 10 A system which limits depth-of-field error due to horizontal beam size.

stop may be put slightly upstream of the image plane.

If the image is to be scanned with a slit, the slit may be tilted with respect to the optical axis so that it is parallel to the image of the line of emission points.

ACKNOWLEDGEMENTS

I wish to thank F. Bulos and H. Wiedemann for reading the manuscript.

REFERENCES

1. R. P. Godwin, 'Synchrotron radiation as a light source,' *Springer Tracts in Modern Physics* (Springer, Berlin, 1969); Vol. 51.
2. A. A. Sokolov and I. M. Ternov, *Synchrotron Radiation* (Pergamon Press, New York, 1968).
3. D. H. Tomboulian and P. L. Hartman, *Phys. Rev.* **102,** 1423 (1956).
4. For example, A. P. Banford, *The Transport of Charged Particle Beams* (E. and F. N. Spon, Ltd., London, 1966).
5. R. A. Mack, 'Spectral and angular distributions of synchrotron radiation,' Report No. CEAL-1027, Cambridge Accelerator Laboratory (1966).
6. See Ref. 1, p. 8.
7. M. Sands, 'The physics of electron storage rings—an introduction,' *Proc. Int. School of Physics, 'Enrico Fermi,' Varenna, Course 46 (1969)*; also Report No. SLAC-121, Stanford Linear Accelerator Center (1970).

Received 30 April 1973;
and in final form 14 June 1973

APPENDIX A

Synchrotron Light Geometry

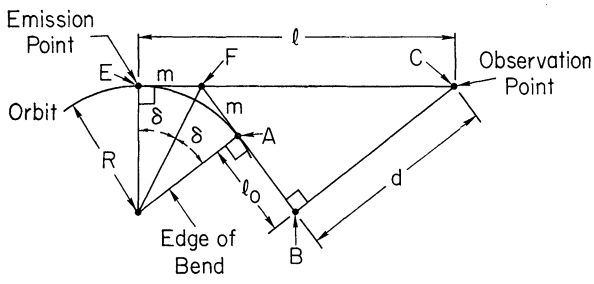

FIGURE 11 Detailed geometry of synchrotron radiation emission and observation.

Referring to Figure 11,

$$l_0 = \overline{AB}$$
$$l = \overline{EC}$$
$$d = \overline{CB}$$
$$m = \overline{EF} = \overline{FA}$$
$$m = R\tan\delta$$
$$\overline{FB} = l_0 + m$$
$$d = \overline{FB}\tan 2\delta$$
$$d = (l_0 + R\tan\delta)\tan 2\delta$$

let $x = \tan\delta$

$$\tan 2x = \frac{2x}{1-x^2}.$$

$$\frac{2x}{1-x^2}(l_0 + Rx) = d$$

finally

$$\tan\delta = \frac{-l_0 - [l_0^2 + d(2R+d)]^{1/2}}{2R+d}.$$

$$l_1 = \frac{d}{\sin 2\delta} + R\tan\delta$$

APPENDIX B

Acceptance Angle Correction

The acceptance angle is $\alpha = s/l$ (refer to Figure 12). The fractional change in acceptance is

$$\Delta\alpha/\alpha = \frac{\Delta d}{l}\cdot\frac{\partial l}{\partial d}$$

for

$$\Delta l = \Delta d(\partial l/\partial d) \ll l.$$

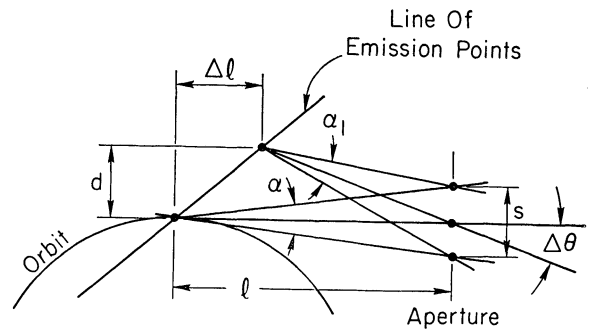

FIGURE 12 The change in acceptance angle due to horizontal orbit distortions.

We shall use the proportionality between Δl and $\Delta\gamma$ to correct the acceptance change. An optical system for correction is shown schematically in Figure 13. The filter at the focal plane of the lens has a transmission profile for light

$$T(x) = \text{power(transmitted)/power(total)} 0 < T \leqq 1$$

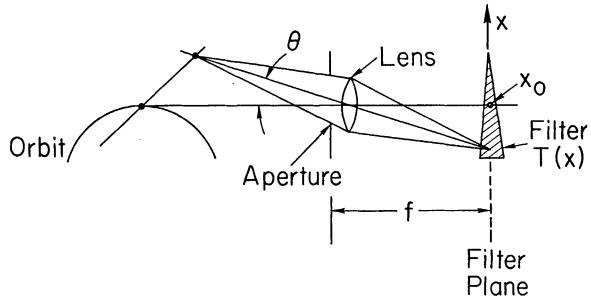

FIGURE 13 An optical system which corrects errors in the angular acceptance of a photometric system due to horizontal orbit distortions.

For an orbit distortion, d, the power at the aperture is

$$P^{(d)} = P\frac{s}{l - d(\partial l/\partial d)}$$

P = power radiated into 1 radian.

The ray passes through the lens and reaches the filter at

$$x = -f\theta = -f\cdot d\cdot(\partial\gamma/\partial d)$$

thus

$$d = -\frac{x}{f}\cdot\frac{\partial d}{\partial\gamma}$$

and $P(d)$ expressed as power variation at the focal plane, $P(x)$, is

$$P(x) = P\frac{s}{l+(x/f)(\partial l/\partial\gamma)}$$

where x is the ray deviation at the focal plane (Figure 13). Now, we posit a constant power passed through the system, independent of d

$$P_0 = P(x)\cdot T(x).$$

P_0 is the power transmitted when $\gamma = 0$, and

$$P_0 = P\cdot T_0\cdot(s/l)$$

$$T_0 = T(x)\,\text{at}\,x = 0.$$

T_0 is arbitrary, and can be chosen for convenience. Then,

$$T(x) = \frac{P_0}{P_x} = T_0 + \frac{T_0 x}{f\cdot l}\frac{\partial l}{\partial\gamma}.$$

APPENDIX C

Correction of the Phase–Space Curvature

We wish to straighten the boundaries of the source area by introducing corrections into the horizontal imaging system, assuming that the horizontal and vertical systems are separable. At the source, the distortion in each ray is an error in x, proportional to θ^2. We need to transform the distribution of rays such that we have errors in θ, proportional x^2, then they can be corrected by a focusing device.

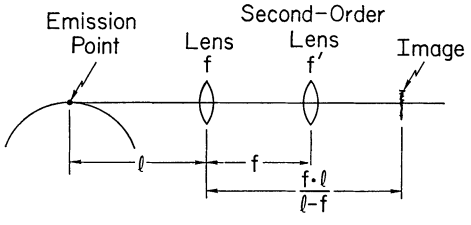

FIGURE 14 An imaging optical system which corrects errors in the horizontal plane due to source curvature.

We use the optical system illustrated in Figure 14. The lens f has focal length f.

The first order transformation matrix for this system, up to f', is

$$T = \begin{pmatrix} 0 & f \\ -1/f & 1-l/f \end{pmatrix}.$$

We work with a single ray from the central trajectory, (X_0,θ_0),

$$x_0 = \tfrac{1}{2}R{\theta_0}^2.$$

In front of f' we have the ray coordinates

$$x = f\theta_0$$

$$\theta = \beta\theta_0 - \frac{x_0}{f} = \beta\theta_0 - \frac{1}{2}\frac{R{\theta_0}^2}{f} \qquad \beta = 1-l/f.$$

If we were imaging a conventional point source instead of the curved central trajectory, $x\equiv 0$, and the second term would be zero. Since the second term is second order in θ_0, we need a second-order lens, which is described by the simplified second-order lens matrix

$$\begin{pmatrix} 1 & 0 \\ -1/k & 1 \end{pmatrix}\cdot\begin{pmatrix} {x_i}^2 \\ \theta_i \end{pmatrix} = \begin{pmatrix} x_f \\ \theta_f \end{pmatrix}$$

where $1/k$ is the strength of the second-order element.

At the exit of the second-order lens we have

$$x = f\theta_0,$$

$$\theta = \beta\theta_0 - \frac{1}{2}\frac{R{\theta_0}^2}{2} - \frac{f^2{\theta_0}^2}{k}.$$

In order to eliminate all second-order terms,

$$\frac{1}{2}\frac{R{\theta_0}^2}{2f} + \frac{f^2{\theta_0}^2}{k} = 0$$

thus

$$k = -2f^3/R.$$

A conventional (first order) thin lens transforms rays such that

$$\theta = -\frac{x_0}{f}.$$

A thin second-order lens has the characteristic

$$\theta = -\frac{{x_0}^2}{k}.$$

This lens may be realized by grinding a reflecting or refracting surface to a third-order curve $Z \propto x^3$ (Figure 15).

We look at the image in its normal position (Figure 14).

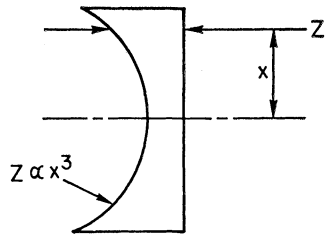

FIGURE 15 A second-order focusing element.